Reorientational transition of the magnetic anisotropy in Co/Cr(001) superlattices

Th. Zeidler, F. Schreiber, and H. Zabel
Institut für Experimentalphysik/Festkörperphysik, Ruhr-Universität Bochum, D-44780 Bochum, Germany

W. Donner
Universität Wuppertal, Fachbereich 8, D-42097 Wuppertal, Germany

N. Metoki
Japan Atomic Energy Research Institute, Tokai-mura, Ibaraki-ken 319-11, Japan
(Received 23 June 1995)

We have measured the magnetic anisotropy of Co/Cr(001) superlattices as a function of the Co thickness using magneto-optical methods and a torsion magnetometer. The samples grown by molecular-beam epitaxy exhibit a reorientational transition of the easy axis from in-plane for large Co thicknesses ($t_{Co} \geq 15$ Å) to out-of-plane for 10 Å $\leq t_{Co} \leq 15$ Å and back again to the in-plane orientation for $t_{Co} \leq 10$ Å. We provide evidence that this reorientational transition of the magnetization direction is due to a sign change of the interface anisotropy constant induced by a concomitant structural phase transition of the Co layers from hcp to bcc with decreasing Co layer thickness.

I. INTRODUCTION

Using advanced growth methods such as molecular-beam epitaxy (MBE) or seeded epitaxial sputtering interfacial effects in heteroepitaxial systems can be studied with unprecedented accuracy. One of the important issues in the field of thin magnetic films is the investigation of magnetic surface or interface anisotropies. For a clear understanding of these anisotropies sharp interfaces and well defined structural properties are of paramount importance.

Perpendicular magnetic anisotropies induced by the interface have been observed for Co/Pd, Co/Pt, and Co/Ru,[1–3] and they are of fundamental interest as well as of highly practical importance in magnetic storage devices. Here we report on the magnetic anisotropy in Co/Cr(001) superlattices in conjunction with the interface-induced structural phase transition of Co on bcc Cr(001). While hcp Co exhibits a perpendicular anisotropy similar to the systems cited above, we have observed a reorientational transition of the easy axis back into the film plane as a result of the interface driven structural phase transition of Co. In this paper we treat the magnetic interface anisotropy of Co/Cr(001) (Refs. 4–6) superlattices, while the interlayer exchange coupling properties will be described in a forthcoming publication.

II. SAMPLE PREPARATION AND STRUCTURAL PROPERTIES

High-quality single-crystal Co/Cr(001) superlattices with Co layer thicknesses of 5–50 Å were grown by molecular-beam epitaxy (MBE) with a base pressure of about $p \leq 5\times10^{-11}$ mbar. The superlattices were grown on a bilayer buffer system consisting of a 500 Å thick Nb(001) layer grown on $Al_2O_3(1120)$ at 900 °C and on top a 500 Å thick Cr(001) layer grown at 450 °C. The growth temperature for the subsequent superlattice was lowered to 300 – 350 °C. All growth temperatures were optimized by x-ray scattering and *in situ* high-energy electron-diffraction (RHEED) measurements. At lower substrate temperatures we observed an island growth mode and at higher temperatures interdiffusion between the adjacent Co and Cr layers occur.

The crystal structure of Co/Cr(001) superlattices has been described in detail elsewhere.[7–10] Therefore in this section we provide a brief summary of the most important structural properties. The structural properties have been investigated by x-ray and RHEED experiments. It was shown that the *c* axis of the hcp Co layers is oriented in the film plane with the Co[0001] axis oriented parallel to the Cr[110] axis. This orientation provides the smallest misfit of about −0.2% and +6% along the Co[00.1] and Co[11.0] axes, respectively. As a consequence of this rather large misfit the epitaxial strain gives rise to a continuous structural phase transition from hcp to bcc with decreasing Co layer thickness. The ideal bcc structure is, however, never realized even down to $t_{Co}=5$ Å. The observed out-of-plane *d* spacing of $d=1.3$ Å for Co(11.0) at $t_{Co} = 10$ Å is too large to be explained by the Poisson expansion from in-plane strains, while it is too small to be taken as evidence for the existence of a metastable bcc phase. Therefore we observe an intermediate structural phase between bcc and hcp in the lower Co-thickness regime. At the same time, the out-of-plane lattice parameter of Cr does not change significantly, indicating that no relaxation processes of the chromium structure takes place with increasing Co thickness. At $t_{Co} = 48$ Å we observe a Co *d* spacing of $d=1.26$ Å close to the bulk value $d=1.25$ Å. The cubic symmetry of Cr(001) causes the existence of two structural domains with the *c* axes of hcp Co perpendicular to each other and aligned parallel to the Cr[110] and Cr[$\bar{1}$10] axis, respectively.

III. EXPERIMENTAL TECHNIQUES

A. MOKE measurements

The magnetic hysteresis curves of the superlattices were measured by the magneto-optical Kerr effect (MOKE). The

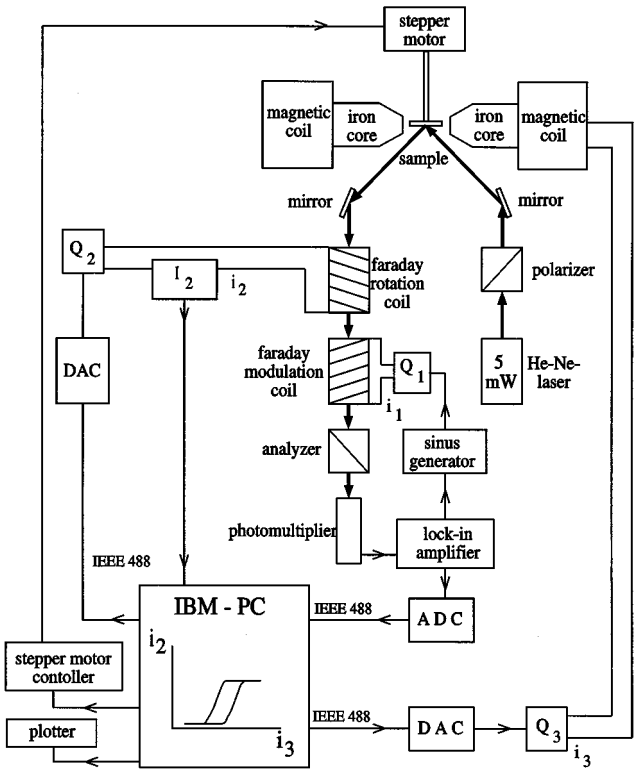

FIG. 1. Schematic view of the experimental arrangement for MOKE. The optical path as indicated by thick arrows represents the longitudinal configuration.

schematic outline of the apparatus is shown in Fig. 1. In the longitudinal configuration the maximum magnetic field is about 10 kOe whereas in the polar case fields up to 18 kOe are available. Using linear polarized light of a nonstabilized He-Ne laser at 632.8 nm and a power of 5 mW the Kerr rotation angle was determined by a high-resolution Kerr magnetometer. The polarization plane is chosen perpendicular to the plane of incidence (*s* state). For the polar case the laser beam passes through a small hole in the magnetic pole with an angle of incidence smaller than 1°. In this configuration the MOKE curves exhibit only the out-of-plane component of the magnetization.

For the longitudinal case we have chosen an angle of incidence of about 45° as shown in Fig. 1. Therefore the longitudinal measurements are sensitive to the in-plane component of the magnetization but any out-of-plane component gives rise to an additional signal and leads to mixed hysteresis curves.

The reflected laser beam passes through the modulator M and the rotator R using the magneto-optical Faraday effect. The extinction axis of the analyzer is parallel to the polarization of the incoming laser beam. The measurement procedure can be described as follows. The modulator M rotates the polarization sinusoidally with an amplitude of $\delta_0 \approx 2.5°$ at a fundamental frequency (FF) of 1 kHz and produces, in first approximation, a first harmonic intensity signal with a frequency of about 2 kHz at the detector. Any Kerr rotation θ_K gives rise to a FF in the detector signal in addition to the first harmonic. The remarkable point here is that theoretical calculations of the apparatus function using the Jones matrix

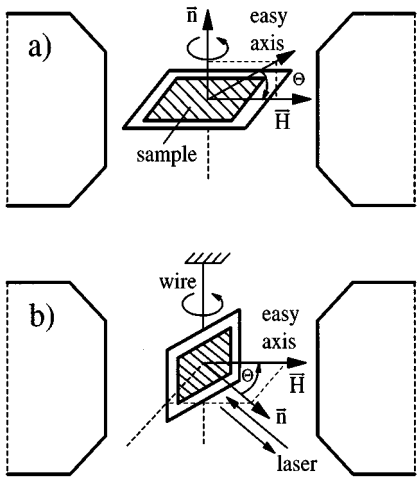

FIG. 2. Schematic arrangement of the sample, electromagnet, and laser beam for easy-axis measurements in a simplified torque magnetometer.

formalism[11] yields an optimal amplitude δ_0 of about 45° for the highest FF intensity. For technical reasons, however, a smaller value of $\delta_0 \approx 2.5°$ was practicable in our setup.

The intensity of the FF was detected by a lock-in amplifier. A certain current I_R applied to the rotator R compensates now the Kerr rotation and eliminates the FF signal. In this case the current I_R is proportional to the Kerr rotation. The eliminating procedure performed at a constant magnetic field provides one measurement point which has to be repeated for different fields to obtain a complete hysteresis loop. The rather high modulation amplitude and the use of lock-in techniques provides an angular resolution of smaller than 10^{-4} degrees.

After measuring a hysteresis loop in the longitudinal MOKE configuration the sample is turned by a certain angle about its surface normal. Repeated measurements of the hysteresis loops for a complete sample rotation provides information on the in-plane magnetic anisotropy.

B. Magnetization measurements

The magnetization of the superlattices was measured by a conventional Faraday balance with magnetic fields up to 14 kOe and gradient fields up to 1 kOe/cm. The measurements were performed with the field oriented parallel or perpendicular to the sample surface to test the saturation state depending on the special properties of the sample as described further below.

Furthermore, using the Faraday balance with homogeneous fields as a simplified ''torque'' magnetometer as shown in Fig. 2, the experimental arrangement allows us to determine the easy axis of the superlattices with arbitrary direction of the remanent magnetization vector. The sample rotates horizontally on a liquid surface such that the in-plane component of the easy axis, i.e., the *c* axis of Co, is aligned parallel to the magnetic field H as indicated in Fig. 2(a). This orientation was then fixed on a glassy sample holder. To determine the out-of-plane component a perpendicular arrangement was used as shown in Fig. 2(b). The angle θ of the easy axis is measured using a laser beam also shown in

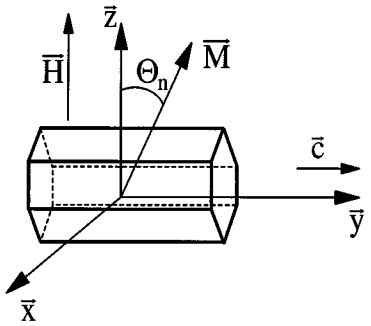

FIG. 3. Geometric configuration of the hcp Co c axis, magnetization **M**, and magnetic field **H** in respect to the sample surface (x-y plane) for model calculations in the polar configuration [Eq. (1)].

the figure. To eliminate any influence from the torque by the attachment wire the position of the sample has to be the same with and without magnetic field.

IV. PHENOMENOLOGICAL MODEL

For the theoretical analysis of the magnetic anisotropy properties of Co/Cr(001) superlattices we have performed absolute minima calculations of the phenomenological anisotropy energy E_A, including Zeeman energy, shape anisotropy, crystal anisotropy terms K_1 and K_2 of Co hcp, and an interface anisotropy K_S. For the polar configuration we use

$$E_A = -\sum_{n=1}^{N} \mu_0 M_S H \cos(\theta_n - \theta_H) + \sum_{n=1}^{N} \frac{1}{2}\mu_0 M_S^2 \cos^2\theta_n + \sum_{n=1}^{N} K_1 \cos^2\theta_n + \sum_{n=1}^{N} K_2 \cos^4\theta_n + \sum_{n=1}^{N} \frac{1}{t_{\mathrm{Co}}} 2K_S \cos^2\theta_n . \tag{1}$$

Here t_{Co} is the thickness of the Co layer.

As shown in Fig. 3 the angle θ_n ($n = 1....N$, $N =$ number of magnetic layers) is defined by the angle between the **z** direction (perpendicular to the surface) and the magnetization **M**. The saturation magnetization M_S of each layer is assumed to be homogeneous. In the polar case the magnetic field H is applied perpendicular to the surface ($\theta_H = 0$). This model is used for the calculation of the crystal anisotropy constants, K_1 and K_2, from the polar hysteresis curves. The validity of this model for Co/Cr(001) is justified further below. For analysis of the in-plane or longitudinal measurements we drop the shape anisotropy term and write

$$E_A = -\sum_{n=1}^{N} \mu_0 M_S H \cos(\phi_n - \phi_H) + \sum_{n=1}^{N} K_1 \sin^2\phi_n + \sum_{n=1}^{N} K_2 \sin^4\phi_n . \tag{2}$$

The in-plane angle ϕ_n is defined by the angle between the Co(00.1) direction and the magnetization. The magnetic field H is applied parallel to the Co(11.0) direction ($\phi_H = \pi/2$).

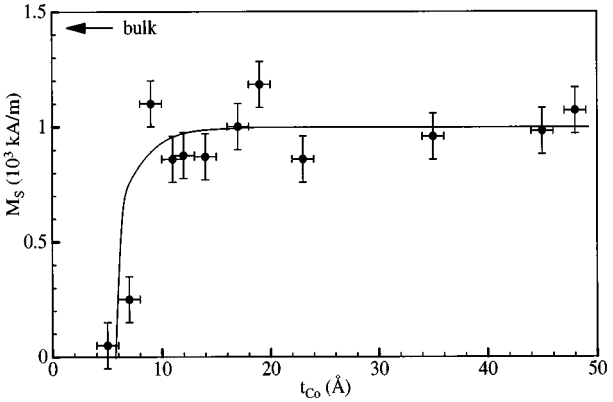

FIG. 4. The saturation magnetization of Co/Cr(001) superlattices is plotted as a function of the Co thicknesses.

In this paper we describe samples which dominantly consist of single Co-structural domains. This simplifies the expressions for the anisotropy energy E_A as written in Eqs. (1) and (2). The case of two crystallographic domains will be treated in a forthcoming paper.

V. EXPERIMENTAL RESULTS

In the following we report on magnetization and anisotropy measurements for Co/Cr(001) superlattices as a function of the thickness of the Co layer. The Cr layer thickness was either kept constant or varied in a thickness range to provide ferromagnetic coupling between the Co layers. The coupling behavior as a function of the Cr thickness will be described in a forthcoming paper. For the superlattices we adopted the following nomenclature: $[\mathrm{Co}_a\ \mathrm{Cr}_b]_c$, where a and b are the individual layer thickness in Å, and c is the number of double layers. All measurements were taken at room temperature.

A. Magnetization

Figure 4 shows the experimental results of the magnetization versus the Co thickness measured by a conventional Faraday balance at room temperature. We have found an average value of $M_S = 1000$ kA/m with an estimated error of 10% for a large range of Co thicknesses. This error arises mainly from the uncertainty in the absolute thickness determination of the superlattices by x-ray scattering. For thicknesses $t_{\mathrm{Co}} > 9$ Å the magnetization of the Co layer reaches a plateau and drops steeply for $t_{\mathrm{Co}} < 9$ Å. In the plateau region the saturation magnetization M_S has an average value of about 1000 kA/m which is smaller than the bulk value of 1440 kA/m. It is well known from the literature[4] that small amounts of Cr drastically reduce the Co magnetization, which drops to zero at a Cr concentration of 25%. In our case and in contrast to earlier results on Co/Cr multilayers[5] we have found no remarkable decrease of the magnetization down to $t_{\mathrm{Co}} = 8$ Å indicating sharp interfaces with interdiffusions not more than 2 Å in the lower Co-thickness regime.

B. Perpendicular magnetic anisotropy

Typical hysteresis curves both for polar and longitudinal MOKE measurements are shown in Fig. 5 as a function of

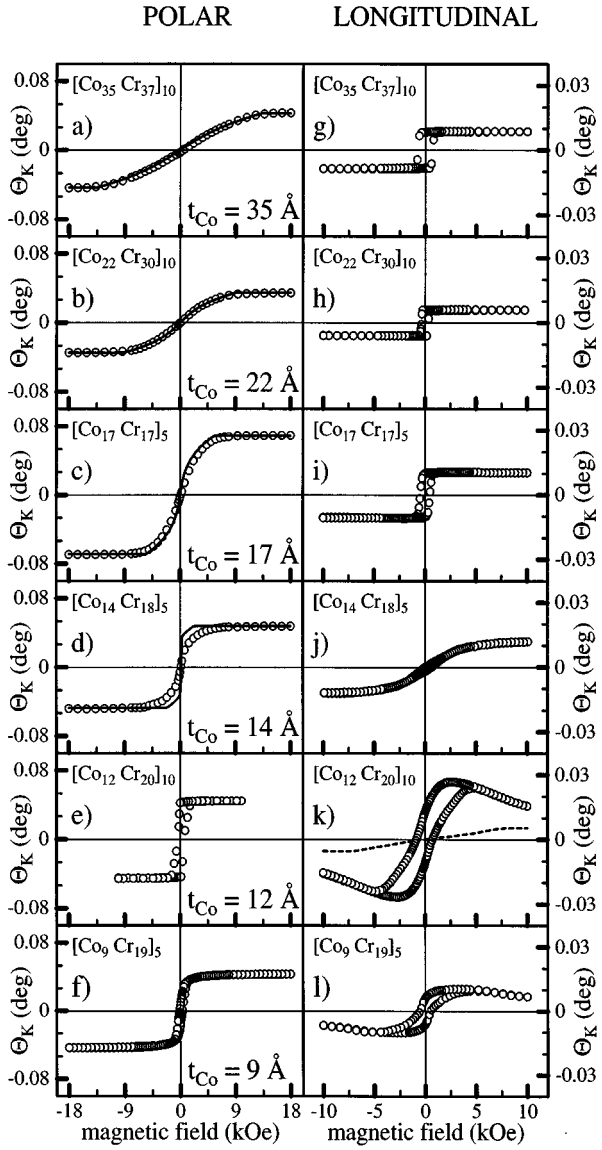

FIG. 5. MOKE hysteresis loops of Co/Cr(001) superlattices as a function of Co layer thickness: (a)–(f) for polar configuration (out-of-plane) and (g)–(l) longitudinal (in-plane) configuration. The solid lines (a)–(d) are fits to the data points using Eq. (1). The hysteresis loop indicated by a broken line (k) is obtained along an orientation intermediated between the in- and out-of-plane orientation. For details see text.

the Co layer thickness. The variation of the Cr layer is of no importance for the following discussion. At large Co thicknesses ($t_{Co} \approx$ 35 Å) we observe a typical hard-axis magnetization curve in the polar configuration [Fig. 5(a)], while in the longitudinal configuration a ferromagnetic easy axis loop occurs [Fig. 5(g)], confirming that the easy axis of magnetization is aligned parallel to the surface.

For decreasing Co thicknesses in the polar configuration the saturation field H_S decreases continuously leading to a typical easy-axis curve for Co thickness down to t_{Co} = 12 Å as shown in Figs. 5(a)–5(d). In this thickness range the longitudinal MOKE measurements exhibit a transition from an easy-axis to a hard-axis-type of hysteresis loop, consistent with the change of the easy-axis direction from parallel into perpendicular orientation with respect to the sample surface.

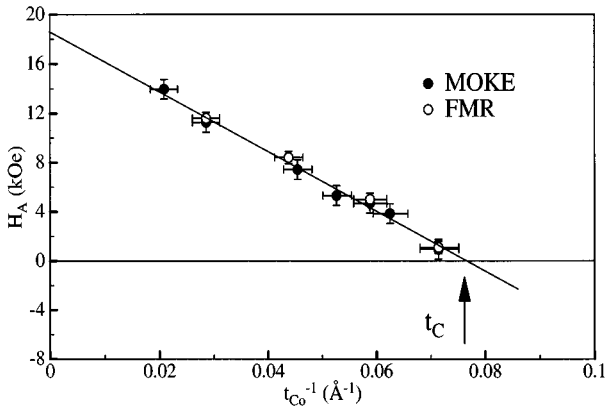

FIG. 6. Effective anisotropy field versus reciprocal Co layer thickness of Co/Cr(001) superlattices measured with FMR and values calculated from longitudinal and polar MOKE measurements using Eq. (3). The solid line is a linear fit to the data with $K_S \approx -0.65$ mJ/m^2 and $t_C \approx 13.5$ Å .

The effective anisotropy field $H_A = 2K_{\text{eff}}/(\mu_0 M_S)$ was determined[12] by the area difference between polar and longitudinal MOKE curves according to

$$H_A = \frac{2}{\theta_K} \int_0^{\theta_K} (H_{\parallel} - H_{\perp}) d\theta_K' . \tag{3}$$

The anisotropy field H_A is plotted versus the inverse Co thickness in Fig. 6. It exhibits a typical $1/t_{Co}$ behavior indicating the presence of a perpendicular interface anisotropy in Co/Cr(001) superlattices with a critical thickness of t_C = 13.5 Å for perpendicular anisotropy. From the slope we obtain an interface anisotropy constant of $K_S \approx -0.65$ mJ/m^2 assuming the reduced saturation magnetization value M_S = 1000 kA/m. This value of K_S is rather large and comparable with the results for Co/Pd (Ref. 1) and Co/Pt.[2] These MOKE data are in a good agreement to recent ferromagnetic resonance studies[12] (FMR) also shown for comparison in Fig. 6. Taking into account the experimental values for K_S and M_S in Eq. (1) we have calculated the magnetocrystalline anisotropy constants K_1 and K_2 by a fit to the data points shown by solid lines in Figs. 5(a) and 5(b). Best results are obtained for $K_1 = 2.1 \times 10^5$ J/m^3 and $K_2 = 1.1 \times 10^5$ J/m^3. These values are in a good agreement with the literature values.[13–15] For t_{Co} = 17 Å a slight disagreement occurs and for decreasing t_{Co} the model used here becomes inadequate.

Now we consider the results for Co thicknesses smaller then 14 Å . The reduced remanent Kerr rotation in Fig. 5(e) indicates that perfect perpendicular alignment of the magnetization is not reached. The corresponding longitudinal MOKE curve [Fig. 5(k)] exhibits a mixture of polar and longitudinal contributions indicating a slanted easy axis with respect to the surface normal. If the magnetic field is applied at an angle of $\theta_H \approx 15°$ as schematically shown in Fig. 7 we observe a typical hard-axis loop as reproduced in Fig. 5(k) by broken lines confirming the slanting easy axis in this direction.

For Co thicknesses smaller than 12 Å we observe a switching of the magnetic moments back into the in-plane orientation. Figure 5(f) shows the polar MOKE curve with a

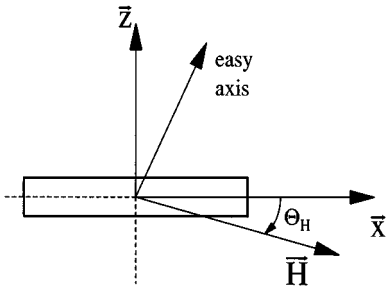

FIG. 7. Schematic arrangement of the magnetic field for a MOKE measurement in the special case of a slanted easy axis. The incoming laser beam is aligned parallel to the **z** axis.

small remanent perpendicular magnetization whereas the corresponding longitudinal MOKE curve reproduced in Fig. 5(l) exhibits mainly an in-plane magnetization with a small perpendicular contribution. This surprising result is very unusual in comparison to other metallic superlattices known at the present time with perpendicular anisotropy such as Co/Pt, Co/Pd, or Co/Ru. This behavior indicates that new anisotropy contributions have to be taken into account at small Co thicknesses.

To shed more light on the origin of the magnetic anisotropy contributions of thin Co layers and to corroborate the MOKE results we have investigated the orientation of the easy axis with respect to the sample normal as a function of the Co thickness. Figure 8 shows the experimental data determined by a simplified ''torque'' magnetometer as described above. The easy axis exhibits a continuous rotation from the in-plane orientation $\theta_M = \pi/2$ for thick Co layers to the perpendicular direction $\theta_M = 0$ with decreasing Co layer thickness at $t_{\mathrm{Co}} = 12$ Å . Significant rotation of the easy axis starts below a Co thickness of $t_{\mathrm{Co}} = 14$ Å without reaching a complete perpendicular orientation. For $t_{\mathrm{Co}} < 12$ Å the magnetic anisotropy rotates back from the perpendicular to the in-plane orientation in good agreement with the MOKE data. We have calculated the easy-axis orientation with the anisotropy model of Eq. (1) setting $H = 0$. The calculated values are shown by the dashed line in Fig. 8. While for large Co

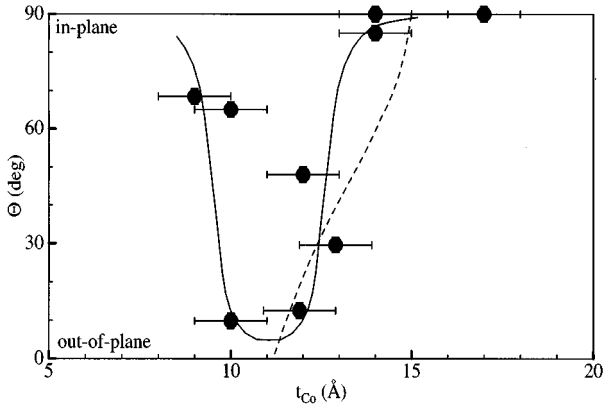

FIG. 8. Easy axis of the magnetization as a function of the Co layer thickness. The solid line is a guide to the eye. The broken line is calculated using Eq. (1) with $H = 0$.

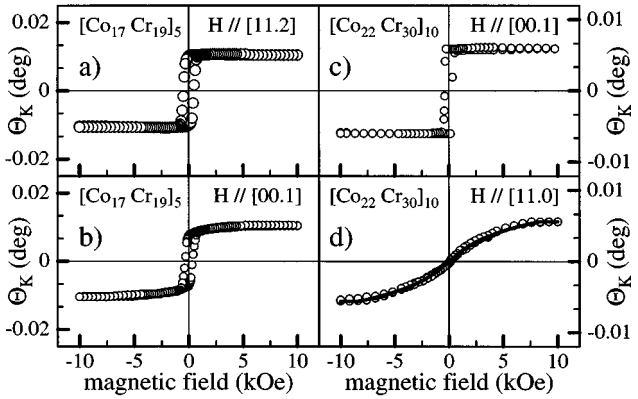

FIG. 9. Longitudinal (in-plane) MOKE hysteresis loops for (a) and (b) fourfold anisotropy (two crystallographic domains) and (c) and (d) uniaxial anisotropy (single-domain structure). The solid line (d) is calculated using Eq. (2) with parameters K_1 and K_2 as used for the polar calculations in Eq. (1).

thicknesses the agreement with the experimental results is satisfactory, at small Co thicknesses the discrepancy between model and experiment is obvious. Normally one would expect from the surface anisotropy term a complete switching of the easy axis from an in-plane to a perpendicular orientation within a thickness range of $\Delta t_{\mathrm{Co}} \approx 2$ Å around the critical thickness. This does not take place here. We come back to this point in the discussion section.

C. In-plane magnetic anisotropy

We have investigated the magnetic anisotropy in the film plane of the Co/Cr(001) superlattices with Co thicknesses down to $t_{\mathrm{Co}} \approx 17$ Å . As mentioned in Sec. II, two types of superlattices may occur either with one or two Co domains. In the case of two structural domains we observe the expected fourfold magnetic in-plane anisotropy as shown in Figs. 9(a) and 9(b), whereas for the single domain case we observe a typical uniaxial anisotropy as shown in Figs. 9(c) and 9(d). Model calculations using Eq. (2) and the values K_1 and K_2 for hexagonal symmetry as determined from the out-of-plane measurements can reproduce well the hard-axis hysteresis curve. In contrast to the strong t_{Co} dependence of the perpendicular anisotropy, for the in-plane case we observe no significant variation as a function of the Co thickness, as shown in Fig. 10.

VI. DISCUSSION

The most remarkable result of the present magnetic anisotropy study on Co/Cr(001) superlattices is the strong Co thickness dependence of the out-of-plane anisotropy. The easy axis changes with decreasing Co thickness from in-plane to out of plane, and then at a Co thickness of about 10 Å back again to the in-plane orientation.

We believe that this rather unusual behavior is strongly affected by the continuous structural phase transition of the Co layers. The experimental results can be explained by a changing interface anisotropy from a negative value for hcp Co and a positive value for Co in the bcc structure preferring an in-plane orientation of the magnetization. As mentioned above, the pure bcc phase was not reached. However, the

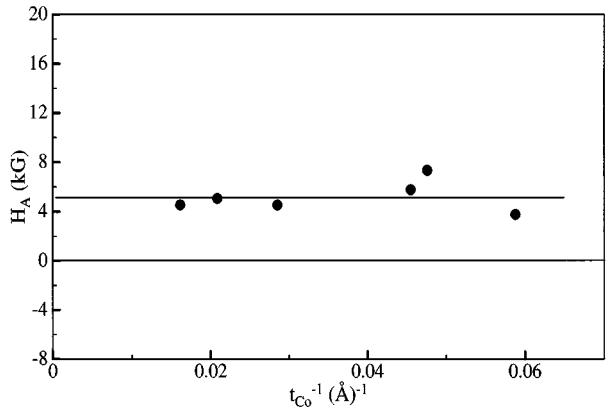

FIG. 10. Effective in-plane anisotropy field versus reciprocal Co layer thickness calculated from in-plane hard-axis and easy-axis MOKE measurements. The solid line is a guide to the eye.

intermediate structure seems to exhibit more ''bcc''-like than hcp-like contributions at the interface. It is well known that the sign of the interface anisotropy is strongly affected by the effective crystal field at the surface[16] either due to the symmetry breaking as predicted by Néel,[17] or due to hybridization effects of the magnetic *d* orbitals by the spacer layer,[18,19] in this case with the Cr atoms at the interface. In our case the interface anisotropy of bcc Co appears to be opposite to the hcp interface anisotropies. This has, however, to remain speculative since the magnetic interface properties of bcc Co are unknown at the present time, except for the predicted ferromagnetic coupling of the bcc Co moments to the Cr moments.[20]

A decreasing magnetic anisotropy in Co/Pt has been explained by an interface roughness of the same order as the Co layer thickness.[1] However, the magnetization of our samples is not significantly reduced down to $t_{Co}= 9$ Å, indicating sharp interfaces and negligible interdiffusion. Furthermore, for $t_{Co}=10$ Å we observe antiferromagnetic interlayer exchange coupling which cannot be reconciled with island growth and pinhole effects. The RHEED streaks observed for this thickness regime also exclude an extensive interface roughness.

The epitaxial strain for the Co layers as mentioned in Sec. II gives rise to strong magnetoelastic contributions to the magnetic anisotropy as described elsewhere.[8] Model calculations according to Mason[21] leads to a perpendicular magnetoelastic contribution of $K_{ME} \approx 6$ kOe using bulk Co hcp elastic and magnetostriction constants and the observed epitaxial strain for $t_{Co} = 10$ Å of about $e_1=7\%$, $e_2 = 3\%$, and $e_3=0.5\%$.[9] Because the strain tensor is assumed to be diagonal we obtain only contributions parallel or perpendicular to the sample surface. Therefore we expect no strain contributions to the observed slanting easy axis.

As to the in-plane anisotropy we expect a transition from a twofold to a fourfold anisotropy according to the Co structural transition from hcp to bcc, respectively. However, in the rather large thickness range of $t_{Co} \geqslant 16$ Å and for the in-plane investigations neither an effect of the phase transition nor of a surface-induced in-plane anisotropy could be detected.

VII. CONCLUDING REMARKS

To summarize we have investigated the in- and out-of-plane magnetic anisotropy in MBE grown Co/Cr(001) superlattices as a function of the Co thickness. All measurements were taken at room temperature. We have observed a strong t_{Co} dependence of the perpendicular magnetic anisotropy causing a perpendicular orientation of the easy axis in the lower Co thickness regime. The easy axis rotates out-of-plane with decreasing Co thickness as a result of the interface anisotropy of hcp Co(1120) on bcc Cr(001). Below $t_{Co} = 10$ Å we observe a reorientational transition of the easy axis back into the Co plane. We believe that this reorientation takes place because of a sign change of the interface anisotropy constant K_S for very small Co thicknesses. This sign change, in turn, may be due to the interface-induced structural phase transition of Co on Cr(001) from hcp to bcc, favoring an in-plane easy-axis orientation. Simulations of the MOKE hysteresis curves are in a good agreement with the experiments both for in-plane and out-of-plane investigations down to $t_{Co} \approx 17$ Å. At lower Co thicknesses our model anisotropy energies are inadequate to describe the hysteresis loops because of strong strain effects and, in particular, because of the structural hcp-bcc phase transition of Co.

ACKNOWLEDGMENTS

We would like to thank J. Podschwadek and W. Oswald for their technical assistance. The work in Bochum was supported by the DFG through SFB 166 ''Structural and magnetic phase transitions.''

[1] B.N. Engel, C.D. England, R.A. Van Leeuwen, M.H. Wiedmann, and C.M. Falco, Phys. Rev. Lett. **67**, 4971 (1991); S.T. Purcell, M.T. Johnson, N.W.E. McGee, W.B. Zeper, and W. Hoving, J. Magn. Magn. Mater. **113**, 257 (1992).

[2] W.B. Zeper, F.J.A.M. Greidanus, P.F. Carcia, and C.R. Fincher, J. Appl. Phys. **65**, 4971 (1991); N.W.E. McGee, M.T. Johnson, J.J de Vries, and J. aan de Stegge, *ibid*. **65**, 4971 (1989).

[3] A. Dinia, K. Ounadjela, A. Arbaoui, G. Suran, D. Muller, and P. Panissod, J. Magn. Magn. Mater. **104-107**, 1871 (1992).

[4] Noburo Sato, J. Appl. Phys. **61**, 1979 (1987).

[5] Y. Henry, C. Mény, A. Dinia, and P. Panissod, Phys. Rev. B **47**, 15 037 (1993).

[6] M.B. Stearns, C.H. Lee, and T.L. Groy, Phys. Rev. B **40**, 8265 (1989).

[7] N. Metoki, W. Donner, Th. Zeidler, and H. Zabel, J. Magn. Magn. Mater. **126**, 397 (1993).

[8] W. Donner, Th. Zeidler, F. Schreiber, N. Metoki, and H. Zabel, J. Appl. Phys. **75**, 6421 (1994).

[9] W. Donner, N. Metoki, A. Abromeit, and H. Zabel, Phys. Rev. B **48**, 14 745 (1993).

[10] N. Metoki, W. Donner, and H. Zabel, Phys. Rev. B **49**, 17 351 (1994).

[11] R.M.A. Azzam, *Ellipsometry and Polarized Light* (North-Holland, Amsterdam, 1977).

[12] If no higher-order contributions ($\sin^4\theta_n$) are relevant.
[13] F. Schreiber, Z. Frait, Th. Zeidler, N. Metoki, W. Donner, H. Zabel, and J. Pelzl, Phys. Rev. B **51**, 2929 (1995); D.M. Paige, B. Szpunar, and B.K. Tanner, J. Magn. Magn. Mater. **44**, 239 (1984).
[14] F. Ono, J. Phys. Soc. Jpn. **50**, 2564 (1981).
[15] Z. Frait, Brit. J. Appl. Phys. **15**, 993 (1964).
[16] U. Gradmann, J. Magn. Magn. Mater. **100**, 481 (1991).
[17] L. Néel, J. Phys. Radium **15**, 225 (1954).
[18] G.H.O. Dalderoop, P.J. Kelly, and M.F.H. Schuurmanns, Phys. Rev. B **50**, 9989 (1994).
[19] D.-S. Wang, R. Wu, and A.J. Freeman, Phys. Rev. B **27**, 15 886 (1993).
[20] F. Herman and P. Lambin, Phys. Rev. B **31**, 4394 (1985).
[21] W.P. Mason, Phys. Rev. B **96**, 304 (1954).